First investigation of the effect of strontium oxide on the structure of phosphate glasses using molecular dynamics simulations

El Mahdi Bouabdalli (bouabdalli.e@ucd.ac.ma)
National School of Applied Sciences, Chouaib Doukkali University, El Jadida https://orcid.org/0000-0002-1140-6837

Mohamed El Jouad
National School of Applied Sciences, Chouaib Doukkali University, El Jadida https://orcid.org/0000-0002-5172-5306

Abdelowahed Hajjaji
National School of Applied Sciences, Chouaib Doukkali University, El Jadida https://orcid.org/0000-0002-4863-4753

Samira Touhtouh
National School of Applied Sciences, Chouaib Doukkali University, El Jadida https://orcid.org/0000-0002-6446-6980

Research Article

Keywords: Phosphate glass, Molecular dynamics, Strontium, Glass network

Posted Date: April 6th, 2022

DOI: https://doi.org/10.21203/rs.3.rs-1522777/v1

First investigation of the effect of strontium oxide on the structure of phosphate glasses using molecular dynamics simulations

El Mahdi Bouabdalli [1,*], Mohamed El Jouad [1], Abdelowahed Hajjaji [1] and Samira Touhtouh [1]

[1]Laboratory of Engineering Sciences for Energy (LabSIPE), National School of Applied Sciences, Chouaib Doukkali University, El Jadida 24000, Morocco.

*Email: bouabdalli.e@ucd.ac.ma

Abstract

Phosphate glasses are characterized by properties distinguished by comparison with those of others such as borates, silicates, and tellurides that can be used in many fields such as optics, electronics, medicine, environmental protection, etc. On the other hand, these pure phosphate glasses have low chemical durability, which limits their application. The addition of strontium to the glass considerably improves its durability. Using classical molecular dynamics simulations, this work investigated the influence of SrO addition on a phosphate glass structure with a nominal chemical composition of (100- x) P_2O_5 – x SrO (where x = 0, 5, 10, 15... 45 mol %). According to the progressive increase in SrO content, the density of the simulated glass increased from 2.400 g/cm^3 to 2.937 g/cm^3, while their molar volume values reduced from 59.143 to 42.449 cm^3/mol. The simulated glasses' short-range structure is described, and it agrees well with prior experimental and theoretical research. Increased SrO level in the glass resulted in phosphate network depolymerization, according to simulations. Furthermore, we evaluated the aggregation parameters of the Sr-Sr pair, and it was most intense for the low SrO content, which can lead to the inhomogeneity of the phosphate glass network.

Keywords: Phosphate glass; Molecular dynamics; Strontium; GLass network.

1. Introduction

In previous decades, many interests have been given to the chemical and physical properties of glass because of its wide variety of properties, which are depending on its composition. In specially, many studies have been made to describe the structure of glasses via several techniques and theoretical studies [1,2]. The phosphate glasses have excellent properties, such as low dispersion and relatively high refractive indices, which compared to the silicate glass, made them good candidates for optical fibers for communication devices [3]. Moreover, phosphate glasses also have other application fields in the biomaterial field [4–8], such as a solid-state laser source [9–12] and for vitrification of high-level nuclear waste [13,14]. In addition, the introduction of rare earth in phosphate glasses makes it attractive in the production of optoelectronic devices [15–18]. However, the phosphate glasses have low chemical durability that provided by the easily hydrated P-O-P bridges leads to their corrosion, induced by water originating, for example, in a humid environment [19,20]. This effect may limit the potential applications for these glasses. The problem can be solved by the addition of alkaline earth such as strontium oxide (SrO), which very strongly increases the glasses' chemical durability [21]. Moreover, the introduction of SrO to phosphate glasses enhances their thermal stability and other physical properties. The incorporation of strontium as a network modifier cation (Sr^{2+}) disrupts the glassy network, which leads to the structure depolymerization and the creation of non-bridging oxygen atoms (Onb), and called terminal oxygen (OT) [3,4,21,22]. As reported in previous studies [23,24] that the numbers of non-bridging oxygens, also named terminal oxygen (OT), increase with more cation oxide content.

The phosphate glass matrix can be described in a convenient method using Q^i notation. Q^i presents a [PO_4] tetrahedron connected by i common oxygen atoms with other [PO_4] tetrahedrons. The bridging oxygen atoms (O_B) are the oxygen atoms bonding two [PO_4] tetrahedrons by P-O_B-P bridges, while the non-bridging oxygen atoms (O_{NB}) are the oxygen atoms connected to only one P. From this, the phosphate glasses can be realized with a range of structures, from a cross-linked network of Q^3 tetrahedra (vitreous P_2O_5) to polymer-like metaphosphate chains of Q^2 tetrahedra to pyro- (Q^1) and orthophosphate (Q^0) anions [1]. There might also be confirmation of non-network oxygen atoms (O_{NN}), which are not bonded to the matrix of the phosphate network and do not participate in their depolymerization [25].

Taking all the above into consideration, this study aimed to explore the effect of SrO substitution on the structural characterizations of glasses with a nominal (100-x) P_2O_5 - x SrO chemical composition, which can be used as optical materials using classical molecular dynamics simulations.

2. Materials and Methods

2.1. Simulation Methods

The classical molecular dynamics has been used to model (100 – x) P_2O_5 – x SrO glasses with various concentrations of strontium oxide (SrO), where x = 0, 5, 10, 15 … 45 mol %. These numerical simulations were performed with the software program DL_POLY_4.09 [26,27]. The aim of the study was explored the influence of strontium on the structure of phosphate glasses with a different composition of (100-x) mol % P_2O_5 – x mol % SrO. This is the (100-x) P_2O_5 - x SrO glass in which part of phosphorus (P) ions was substituted by different contents of strontium (Sr). For all simulations, the numbers complete of atoms comprised between 11570 and 14336 ions and were randomly placed in an orthorhombic simulation box for various configurations of the models. The exact formal compositions of strontium contained in phosphate glasses are described in Table *1*. The box lengths were set according to the experimental glass density. To remove the surface effects, periodic boundary conditions were applied.

The pair interactions of i-j ions were described using the Buckingham potential of the equation:

$$V\left(r_{ij}\right) = \frac{q_i q_j}{4\pi\varepsilon_0 r_{ij}} + A_{ij}\exp\left(\frac{-r_{ij}}{\rho_{ij}}\right) - \frac{C_{ij}}{r^6{}_{ij}} \quad (1)$$

Where V (r_{ij}) is the Buckingham potential of i-j ions, r_{ij} is the distance between ions i-j, ε_0 is the permittivity of free space, q_iq_j is the product of effective charges, and A_{ij}, ρ_{ij} and C_{ij} are parameters given in Table 2, which were taken from literature [28]. The first term of the Eq. (1) is responsible for coulombic interactions; the second term is responsible for repulsion interactions and last determine Van der Waals forces.

Table 1: Simulated compositions (in mole %) and their densities and cell sizes.

Samples	P_2O_5	SrO	Densité (g/cm^3)	Number of atoms	Cell zise ($Å^3$)
PSr0	100	0	2.400	14336	352.146
PSr5	95	5	2.444	13967	352.146
PSr10	90	10	2.491	13721	352.146
PSr15	85	15	2.542	13415	352.146
PSr20	80	20	2.596	13106	352.146
PSr25	75	25	2.654	12800	352.146

PSr30	70	30	2.717	12494	352.146
PSr35	65	35	2.784	12185	352.146
PSr40	60	40	2.858	11879	352.146
PSr45	55	45	2.937	11570	352.146

The Buckingham potential is very beneficial for describing the mostly ionic interactions. For more covalent bonds, the three-body term is essentially used to describe the directional character of the bonds. The P-O bond has a strongly covalent character; therefore, the three-body potential was used to determine O-P-O and P-O-P interactions [29] :

$$V_{iji}(\theta) = \frac{1}{2}K_{iji}\left(\theta_{iji} - \theta\right)^2 \quad (2)$$

Where j is the type of element of the central atom, k_{iji} is the three-body force constant, θ_{iji} is the reference bond angle and θ is the bond angle for O-P-O and P-O-P interactions. Potential parameters of the three body are listed in Table 3.

Table 2: Values of the Buckingham potential parameters of the i-j pair [28].

Pair (i-j)	A_{ij} (eV)	ρ_{ij} (Å)	C_{ij} (eV.Å^6)
Sr – Sr	16574.664	0.2600	0.0000
Sr – O	2026.613	0.3100	0.0000
P – P	831.250	0.3000	0.0000
P – O	887.340	0.3700	0.0000
O – O	454.343	0.3600	0.0000

Table 3: Values of the parameters used to calculate the potential in equation 2.

Triplet (i-j-i)	Kiji (ev)	θ_{iji}(°)
P-O-P	3.0	135.5
O-P-O	3.5	109.47

The common simulation procedure was used to produce the modeled glass structures: an initial configuration is first melted at 10000 K for 0.01 ps to ensure a perfect mixing of the system. After that step, the melts are gradually cooled to room temperature (300 K) with a quenching rate of 10 K/ps. The glassy structures are finally relaxed at room temperature for 0.01 ps. During the latter stage, the structural parameters are sampled for further analysis (see Figure 1).

3. Results and Discussion

3.1. Density

The dependencies of the density and molar volume of the simulated strontium phosphate glasses are shown in Figure 2. Linear functions of the density of the simulated glass in the Figure 2 have been fitted using linear regression. The glass density increased linearly with increasing SrO content according to the formula $\rho(x) = (0.0118\ x + 2.3757)$ (g / cm^3) and $R^2 = 0.991$. The obtained value of the glass density for the composition x = 0 (2.3757 g/cm^3) is in good agreement with the experimental value obtained, which is equal to 2.32 g /cm^3 for the same glass composition as reported in [21].

More information concerning the glass network changes can help determine the molar volume.

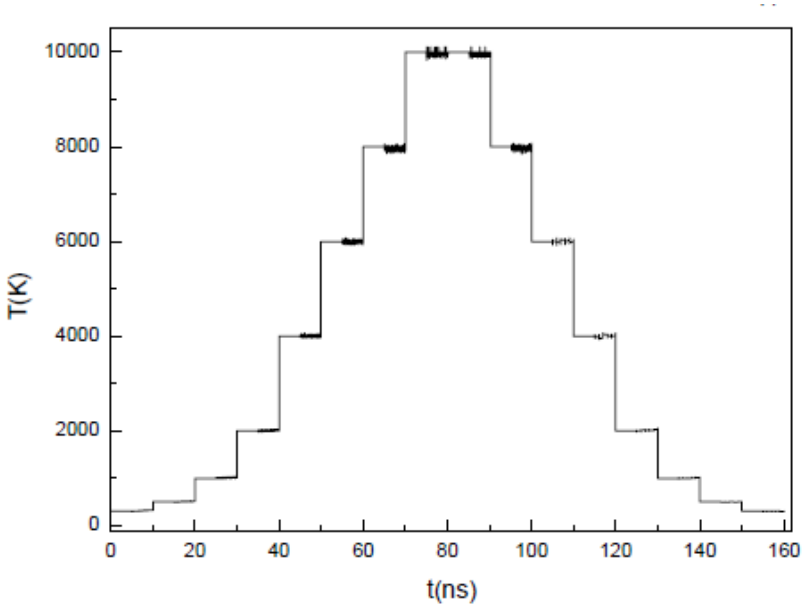

Figure 1: Temperature evolution during heating and cooling

The molar volume was calculated according to the formula V = M/ρ, where ρ is the glass density and M is the molar mass of the glass. The calculated values of the glass molar volume are also included in Figure 2. The molar volume decreased according to the formula V (x) = -0.37097 x + 59.14355 (cm^3 / mol). The decreased value indicated that the glass network had become more compacted. This can have been associated with the placement of the Sr atoms in the open voids of the glass network; in this way, the free space of the network would have decreased. This result strongly indicates the modifier role of strontium in the glass network. These results agree well with those of the previous work [21].

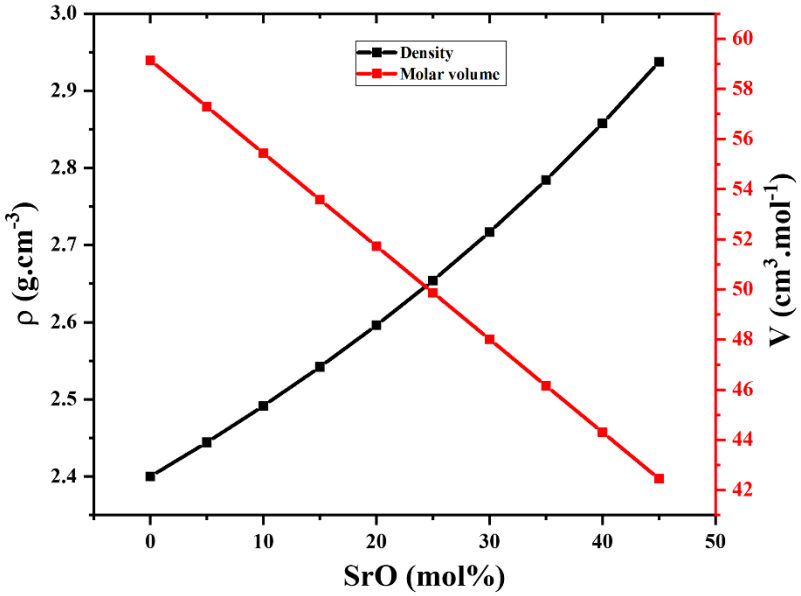

Figure 2: Density and molar volume of the simulated glass as a function of the content of strontium oxide.

3.2. Modeled structures of some simulated glasses

The views of the pure and doped phosphate simulated structures with some content of strontium oxide are shown in Figure 3. It clearly appears that the strontium atoms are homogeneously distributed in the phosphate glass matrix.

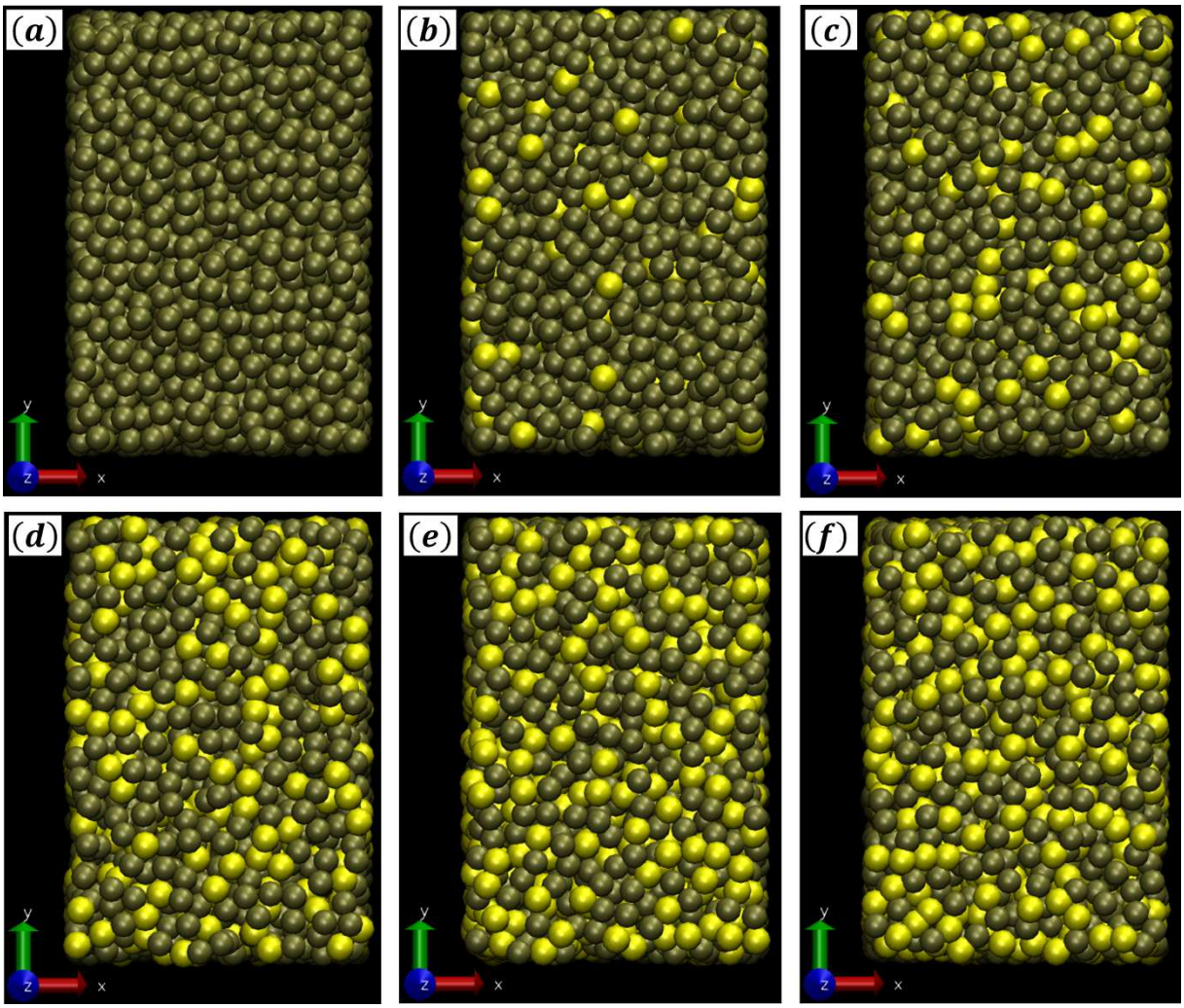

Figure 3: Views of the simulated phosphate structure (a) and the simulated phosphate structure doped with some SrO content: 10 mol % (b), 20 mol % (c), 30 mol % (d), 40 mol % (e) and 45 mol % (f). Color code : Phosphorus is gray, and strontium is yellow.

3.3. Partial radial distribution function

The partial distribution function (PDF) is defined as a function that is used to describe the features of the short-range order in the glasses. Moreover, the PDF also defines the variation of the probability density as a function of the distance from a specified particle. The formula for the PDF is given by the following equation:

$$g_{ij}(r) = \frac{V}{N_i N_j} \sum_j \frac{n_{ij}(r-\Delta r/2, r+\Delta r/2)}{4\pi r^2 \Delta r} \quad (3)$$

Where V is the volume of the simulation cell and Ni and Nj are the total numbers of ions i and j, respectively. The term $n_{ij}(r - \Delta r/2, r + \Delta r/2)$ is the average number of ion j surrounding ion i within the distance of r ± r/2. Exemplary PDF curves for P-O, Sr-O, and O-O pairs for x = 25 mol % glass are presented in Figure 4.

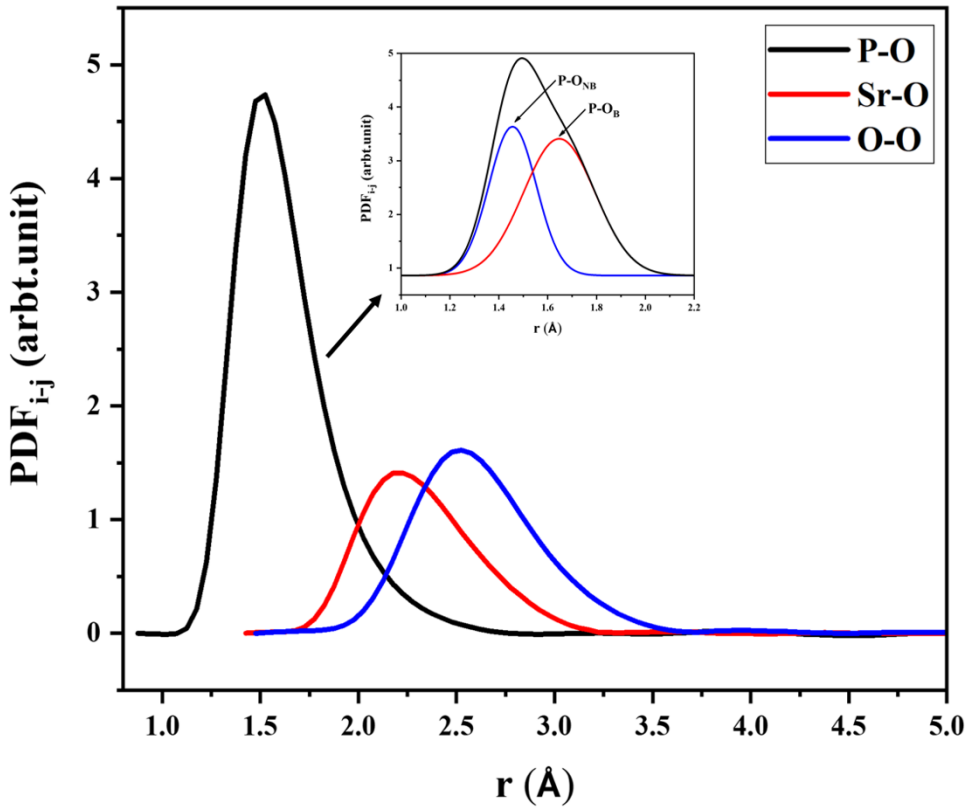

Figure 4: The P-O, Sr-O, and O-O pair distribution functions (PDFs) for 25-mol% of SrO

As would be expected for amorphous systems, the obtained curves were characterized by a single well-developed peak that as the influence of the short-range order in the closest coordination shell. The other peaks were significantly less intense that confirm the glassy character of the simulated systems. For the rest of the tested systems, the found curves were very similar. It must be indicated that the first PDF peak for the P-O pair was composed two peaks (as presented in Figure 4), which were attributed to two main P-O bond lengths that are depending on the role of oxygen in the [PO_4] tetrahedron. The first peak of the lower P-O length was attributed to shoter P-O_{NB} bonds, which the maximum located at ca.1.456 Å. This lastly value is a good agreement with the literature data, which the bond length is in the region of 1.43–1.49 Å [30]. The P-O_{NB} bond length increased linearly with the concentration of strontium oxide, as shown in Figure 5 (P-O_{NB} curve). This increase may be assigned to the increased content of P-O_{NB} bonds compared to P-O_B bonds. The P-O_B bond lengths are longer than the P-O_{NB} bond lengths [31]. Consequently, with increasing of the P-O_{NB} content, the position of the PDF curve component moves toward higher lengths. The influence may also be because the strontium (Sr) ions prefer to break double P-O_{NB} bonds and transform them into P-O_{NB}-Sr joining, instead of disrupting P-O_B-P bridges. However, the P-O_B bond length was higher and the proportionate component of the first PDF peak was located for greater distances. The position of the peak was composed of 1.62 and 1.67 Å and was almost constant. The P-O_B distances are in good agreement with the previous MD results indicating ca. 1.51–1.64 Å [1,31–35]. However, it should be noted that the MD values are higher than the values from ab initio

simulations, which are closer to 1.6 Å [31,36–38]. This may be an effect of the simulation model and the P-O interatomic potential parameters used.

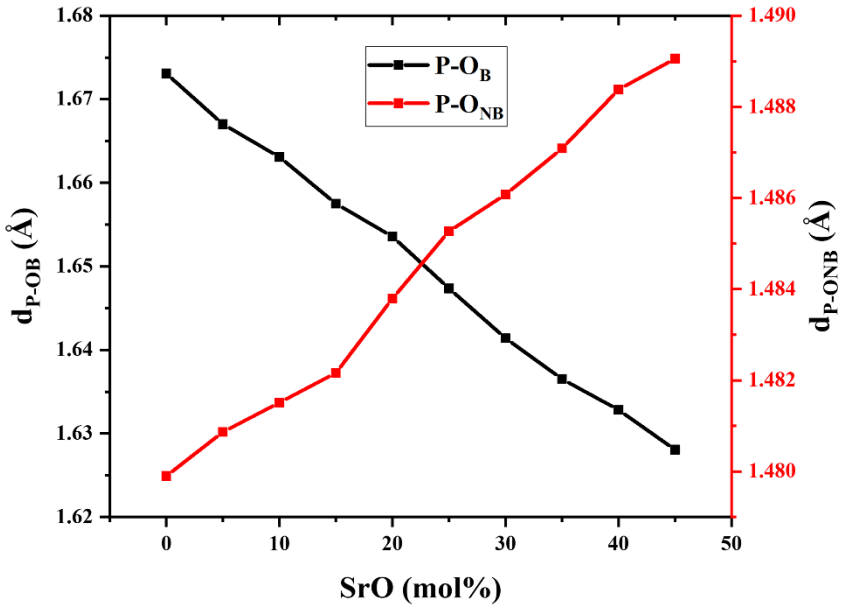

Figure 5: Variation of P-O$_B$ and P-O$_{NB}$ bond lengths the simulated glasses as a function of the content of strontium oxide.

3.4. Coordination Number Analysis

The coordinate number of the given central atom at the distance is obtained by integrating the PDF curve. Thus, the integration donates the average coordination number (CN) of P to oxygen according to the distance from the central P atom. The obtained CN curves are represented in Figure 6. The coordination number of the P atom appeared as a step-like curve, which is characteristic of glass network formers [30]. The P atoms are taken, in a step-like manner, and have a constant coordination number of 4 compared to oxygen. Furthermore, the value of the assumed cut-off radius was freed in a large range from above 1.7 Å up to ca. 2.8 Å. This proved that all phosphorus atoms were located in the middle of the oxygen tetrahedrons [PO_4]. Above 2.8 Å the second coordination sphere started. However, the coordination number curves for Sr and O do not have the characteristic step-like manner. The form of these curves is mainly the feature for the glass network modifiers.

The variation in the coordinate numbers for P, Sr, and O in relation to oxygen as a function of the content of strontium oxide is presented in Figure 7. The average coordination numbers for the pairs P-O, Sr-O and O-O were determined using the cutoff radiuses following (rc): 2.647, 3.356, and 3.757 Å, respectively. It is mentioned that these values were taken between the first and second maximums of the appropriate PDF functions, which mainly present the minimum. As seen in Figure 7, the number of P coordination decreases and increases in Sr with increasing strontium oxide content in the glass composition. In addition, the number of P coordination is slightly higher compared to the values obtained in the earlier study, which ranged from 4.008 to 4.013 [39]. However, the coordination number of Sr increases from 7.237 to 7.916 when the content of strontium oxide increases from 5 to 45 mol%, which is good according to previous molecular dynamic simulations [40]. Furthermore, the average number of O coordination

decreases from 11.586 to 9.219 when the strontium content increases in the glass simulated composition as seen in Figure 7.

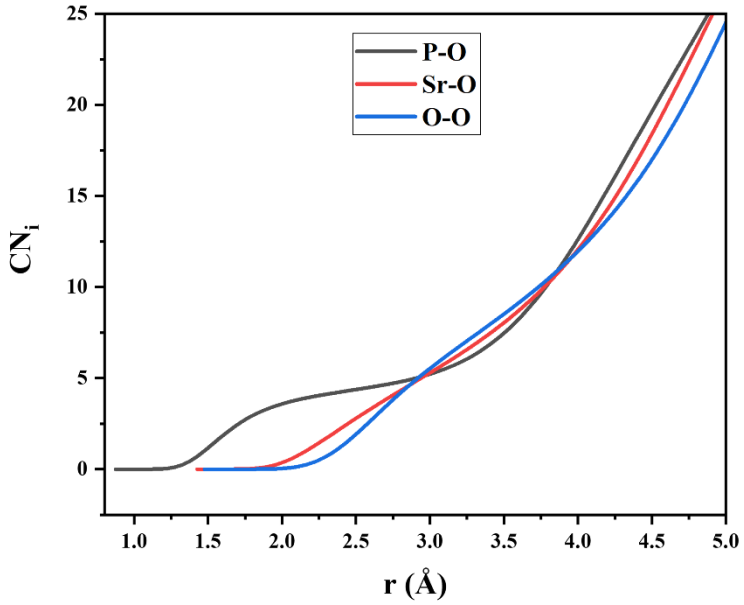

Figure 6: The coordination number of the pair P-O, Sr-O, and O-O as a function of the distance for the simulated glasses containing 25-mol% of SrO.

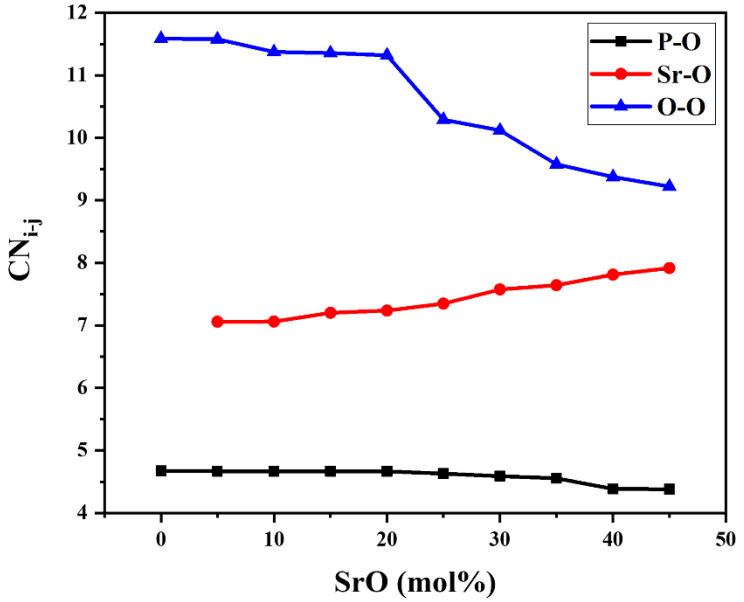

Figure 7: The P-O, Sr-O, and O-O coordination number as a function of the glass composition.

In addition, Figure 8 shows the Sr-O distance and the coordination number of the simulated glass as a function of the strontium oxide content. We observed that the longest distance was the Sr-O distance that increased with increasing SrO content in the phosphate glass, and at the same time, the number of coordination with respect to oxygen also increased from 7.237 to

7.916. The increase in the Sr-O distance and the coordination number in the simulated glass with the SrO content is in good agreement with those previously studied, as reported in [40,41].

In general, we can find that the increase in the content of strontium oxide (SrO) in phosphate glass increased the mean coordination numbers for oxygen for the form of strontium and decreased for the form of phosphorus. The increase in the number of Sr-O coordination was related to the extension of the mean distances from oxygen. In this case, this linear growth proved the relationship between the distance and the coordination number. In addition, we might suppose that the chemical bond lengths followed the trend. A similar conformation has been observed for calcium atoms in phosphate glasses as reported in [30].

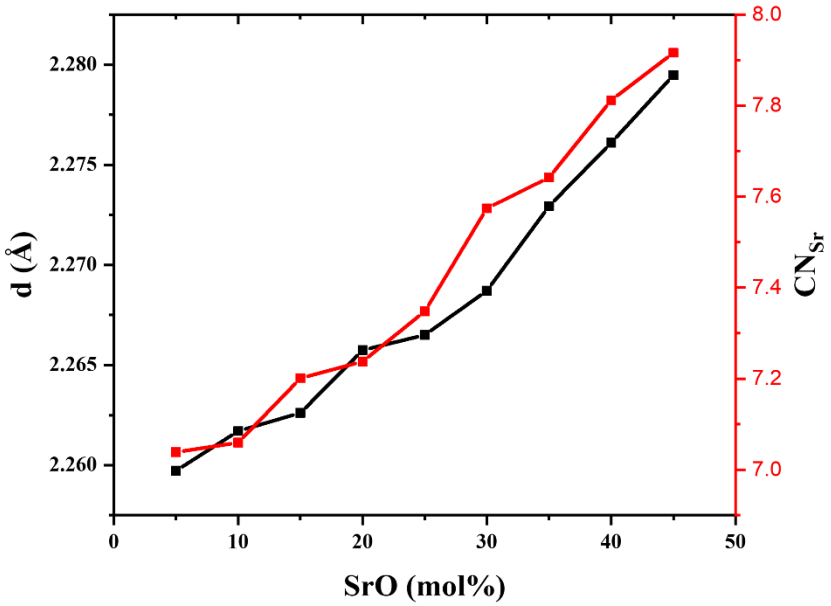

Figure 8: Dependence of the Sr-O distance and coordination number as a function of the content of SrO in the glass composition.

3.5. Angle distribution function

In the simulated systems, phosphorus pentoxide (P_2O_5) was the only pure oxide of the network. Consequently, in the further description of the glass network, we concentrate principally on this cation. The P-O-P and O-P-O angle distribution functions (ADFs) are important parameters that describe the network. The ADFs for the simulate glasses are shown in Figure 9 and Figure 11.

The angle of the P-O-P bond is the angle at which the [PO_4] tetrahedrons are connected by each other. In this study, the distribution was more largely due to a much higher level of randomness. The position of the maximum angle of P-O-P linearly decreased with increasing strontium oxide (SrO) in the composition glass, which might have been an influence of the phosphate chains' shortening. This behavior is in good agreement with those previously studied [42]. In addition, the full width at half-maximum (FWHM) of the P-O-P bond also increased with increasing the content of SrO as observed in Figure 12. However, the angle of the O-P-O bond describes the angle of the bond in [PO_4] tetrahedrons. In an ideal tetrahedron, the distribution would typically have a maximum for an angle of 109.47 °, and a similar maximum was observed in these simulated glasses. The potion of the maximum O-P-O angle was dependent on the glass composition. Thus, the intensity of the peak slightly decreased with the content of strontium

oxide, as seen in Figure 11. Furthermore, the maximum angle of position of O-P-O increased with the content of SrO and its full width at half maximum (FWHM) also decreased, as shown in Figure 10. The values of the average bond angles of O-P-O and P-O-P are comparable with the values obtained previously 107°-110° and 151°-160°, respectively [32,43].

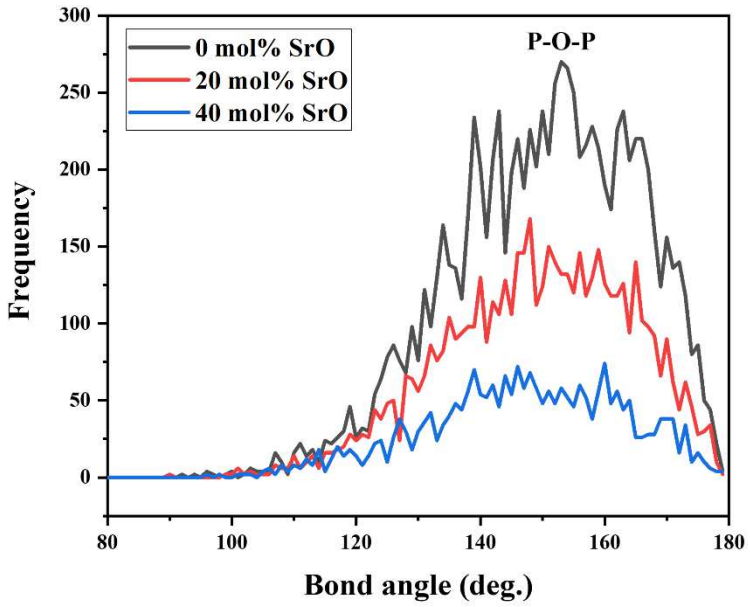

Figure 9: The angular distribution function of P-O-P bonds for the glasses.

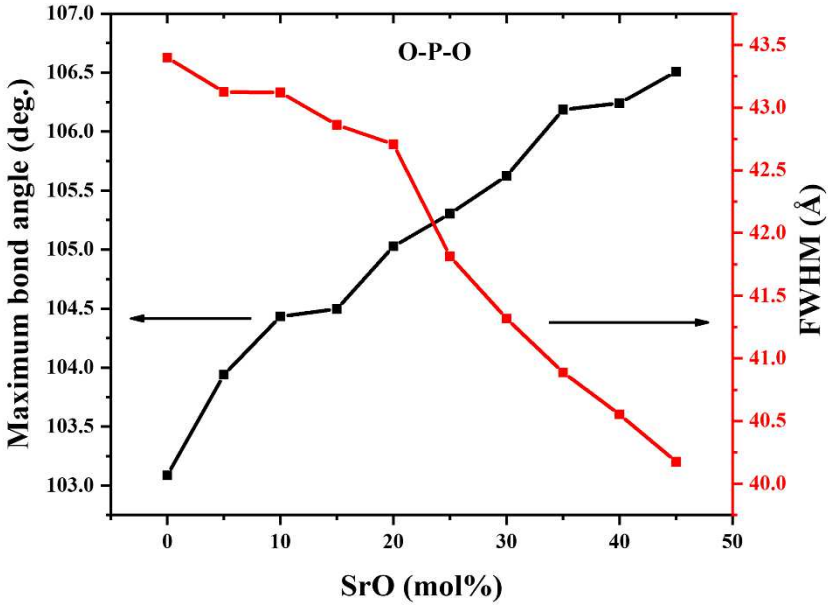

Figure 10: Dependence of the maximum angle and FWHM of the O-P-O bond on the SrO content in the glass composition.

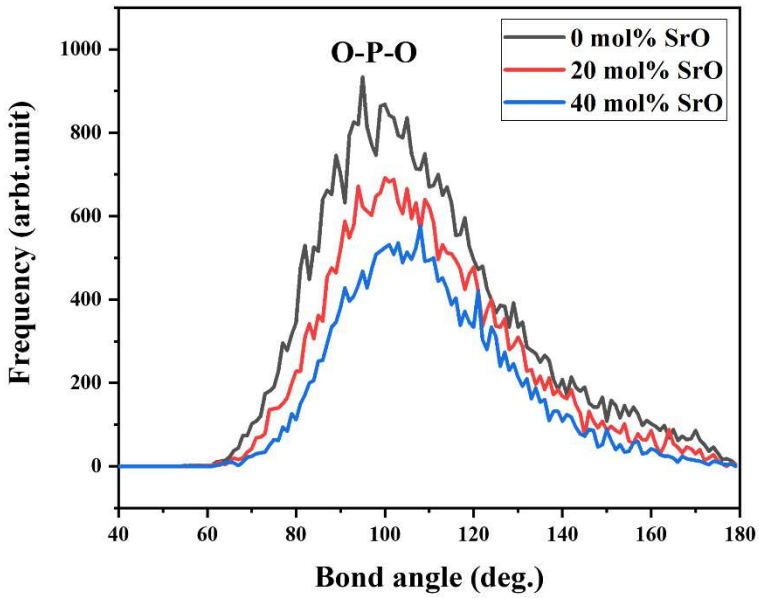

Figure 11: The angular distribution function of O-P-O bonds for the glasses.

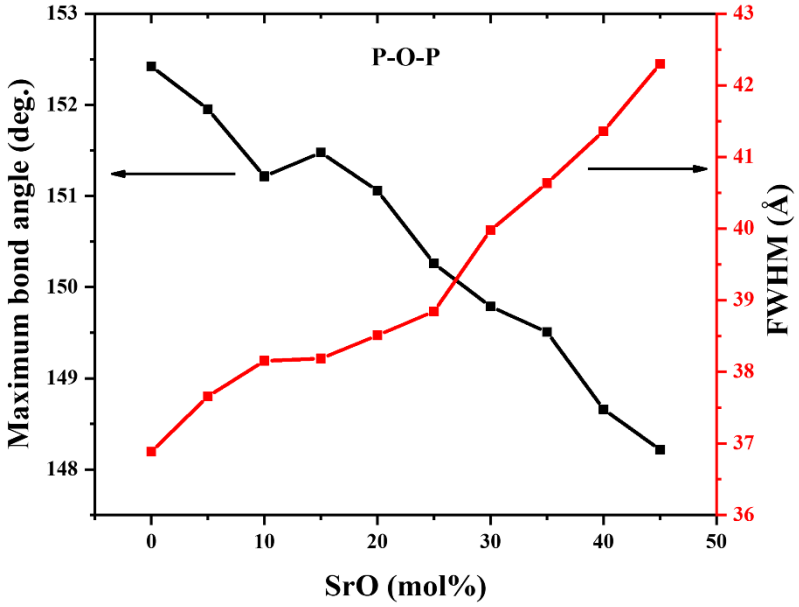

Figure 12: The maximum angle and FWHM of the P-O-P bond as a function of the SrO content in the glass composition.

3.6. Distribution of Q^n for the different sample

The Q^i notation can study the changes in the structure of the glass network appropriately. The distribution of the Q^i structural units in the simulated glasses according to the glass composition is presented in Figure 13. The base glass network is mainly made up of Q^3 with some comparable additions of structural units Q^2 and Q^1. Therefore, the matrix of the phosphate network consisted of long chains, connected to each other by Q^3 units and finished by Q^1 units. As seen in Figure 13, the introduction of strontium oxide (SrO) in the phosphate glass led for

the first time to a decrease in the number of structural units Q^3. Consequently, the joined chains were being separated. Second, the decrease in Q^2 structural units became more rapid with a higher content of strontium oxide. In parallel, there is the formation of the structural units, Q^1 and Q^0, which replace the structural unit Q^3. Therefore, in the middle region of the SrO content in the phosphate glass, the longer chains were shortened and again separated Q^0 units were distinguished. The high modifier content in the glass was built of very short chains, such as Q^1 units and separated Q^0 units. The results of the depolymerization of the simulated glass by the strontium oxide modifier are in good agreement with those obtained experimentally for some similar composition of the network glass, which are confirmed by the infra-red (IR) and Raman spectra that show the role of the network modifier of Sr^{2+} ions and also demonstrate that the structural network of these phosphate glasses comprises branching (Q^3), middle phosphate tetrahedra (Q^2) and pyrophosphate (Q^1) and finally isolated entities (Q^0) [21].

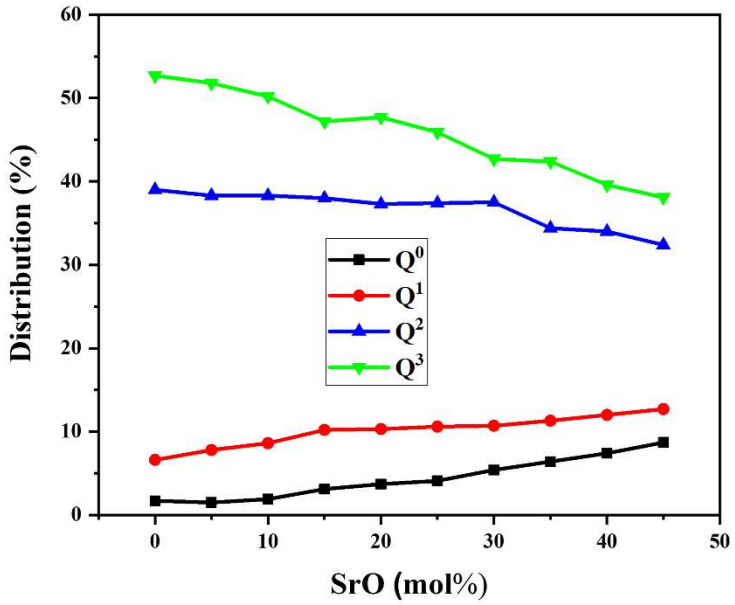

Figure 13: Distribution of Q^i structural units in the simulated glasses.

3.7. Clustering

From the calculated values of the coordination numbers of the Sr-Sr pair, we used them to obtain the aggregation parameters (R_{Sr-Sr}), as defined in [44]. This parameter was defined as a simple ratio of the coordination number to a homogeneous random distribution. A value above 1 designated ions clustering. The evaluated values of the aggregation parameter (R_{Sr-Sr}) are presented in Figure 14. As seen in the last figure, we observed that the values of the parameter demonstrate that, with a low content of strontium oxide (SrO), a very strong aggregation of the atoms can be observed. This leads to the formation of Sr-rich clusters and does not result in the homogeneity of the glass structure. The increase in the SrO content in the phosphate glass composition induced an increase in the regions, and, in this method, the complete phosphate glass network became more homogeneous. A similar influence was observed for Ca [30]. However, in the state of Ca, the value of the aggregation parameter was lower and, for the low modifier, the contents were about twice the Ca value. Therefore, we concluded that the aggregation of Sr was stronger than that of Ca.

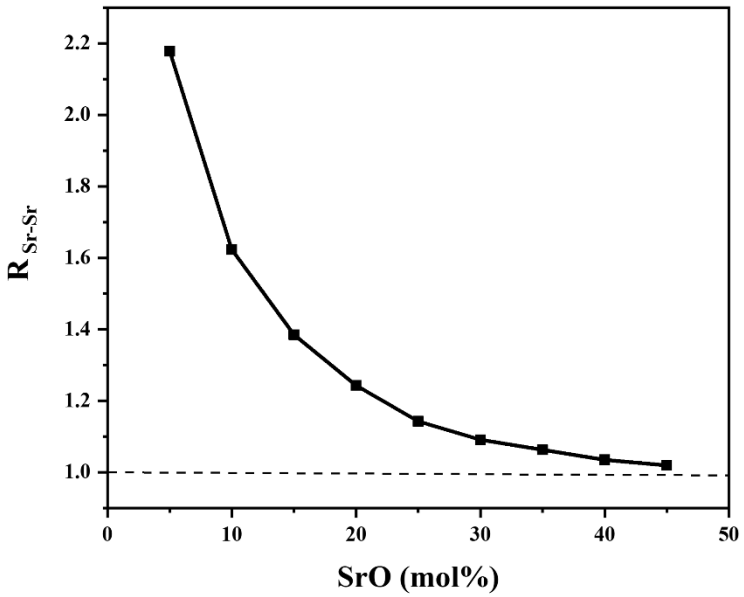

Figure 14: Variation of the Sr-Sr aggregation parameter (Rsr-sr) of the glass composition as a function of the SrO.

4. Conclusion

In conclusion, we have discovered the effect of the SrO on the structural properties of phosphate glasses with their different content using classical molecular dynamics simulations. The density of the simulated phosphate glasses increases from 2.400 g/cm^3 to 2.937 g/cm^3 with increasing SrO content, which is in good agreement with the previous experimental study. The increasing content of SrO in phosphate glass is accompanied by an increase in the bond lengths of P-O_{NB} and Sr-O, but the bond length of P-O_B decreases with this content of SrO. We have found that the number of coordination of the Sr-O pair increases from 7.057 to 7.915 and decreases for the P-O pair from 4.673 to 4.379, respectively, with increasing SrO content. The simulated phosphate glasses with low strontium oxide contents were built of chains, which can have branches and form three-dimensional structures. The increase in SrO content in the phosphate glass led to its network depolymerization, which was characterized by transforming the longest chains of structural unit Q^3 to pyrophosphate (Q^1) and isolated entities (Q^0). This result corresponded well with that obtained experimentally. We calculated the strontium aggregation parameters, and it was primarily intense because of the low SrO contents. This result can lead to non-homogeneity of the glass network with the formation of Sr-rich and Sr-depleted regions.

Acknowledgments

The National Center for Scientific and Technological Research, Rabat / Morocco, has supported this research.

Reference

[1] Brow RK. Review: the structure of simple phosphate glasses. J Non Cryst Solids 2000;263. https://doi.org/10.1016/S0022-3093(99)00620-1.

[2] Hoppe U, Kranold R, Barz A, Stachel D, Neuefeind J, Keen DA. Combined neutron and X-ray scattering study of phosphate glasses. J Non Cryst Solids 2001;293–295:158–68.

https://doi.org/10.1016/S0022-3093(01)00666-4.

[3] Kerkouri N, Haddad M, Et-Tabirou M, Chahine A, Laânab L. FTIR, Raman, EPR and optical absorption spectral studies on V2O5-doped cadmium phosphate glasses. Phys B Condens Matter 2011;406:3142–8. https://doi.org/10.1016/J.PHYSB.2011.04.057.

[4] Pascuta P, Borodi G, Jumate N, Vida-Simiti I, Viorel D, Culea E. The structural role of manganese ions in some zinc phosphate glasses and glass ceramics. J Alloys Compd 2010;504:479–83. https://doi.org/10.1016/J.JALLCOM.2010.05.147.

[5] Pascuta P, Borodi G, Popa A, Dan V, Culea E. Influence of iron ions on the structural and magnetic properties of some zinc-phosphate glasses. Mater Chem Phys 2010;123:767–71. https://doi.org/10.1016/J.MATCHEMPHYS.2010.05.056.

[6] Mansour E, El-Damrawi G. Electrical properties and FTIR spectra of ZnO–PbO–P2O5 glasses. Phys B Condens Matter 2010;405:2137–43. https://doi.org/10.1016/J.PHYSB.2010.01.121.

[7] Knowles JC. Phosphate based glasses for biomedical applications. J Mater Chem 2003;13. https://doi.org/10.1039/b307119g.

[8] Abou Neel EA, Knowles JC. Physical and biocompatibility studies of novel titanium dioxide doped phosphate-based glasses for bone tissue engineering applications. J Mater Sci Mater Med 2008;19. https://doi.org/10.1007/s10856-007-3079-5.

[9] Tischendorf B, Otaigbe JU, Wiench JW, Pruski M, Sales BC. A study of short and intermediate range order in zinc phosphate glasses. J Non Cryst Solids 2001;282:147–58. https://doi.org/10.1016/S0022-3093(01)00350-7.

[10] Walter G, Hoppe U, Vogel J, Carl G, Hartmann P. The structure of zinc polyphosphate glass studied by diffraction methods and 31P NMR. J Non Cryst Solids 2004;333:252–62. https://doi.org/10.1016/J.JNONCRYSOL.2003.12.054.

[11] Ravikumar RVSSN, Ikeda K, Chandrasekhar A V., Reddy YP, Rao PS, Yamauchi J. Site symmetry of Mn(II) and Co(II) in zinc phosphate glass. J Phys Chem Solids 2003;64:2433–6. https://doi.org/10.1016/S0022-3697(03)00286-5.

[12] Hudgens JJ, Brow RK, Tallant DR, Martin SW. Raman spectroscopy study of the structure of lithium and sodium ultraphosphate glasses. J Non Cryst Solids 1998;223:21–31. https://doi.org/10.1016/S0022-3093(97)00347-5.

[13] Sales BC, Boatner LA. Lead-iron phosphate glass: A stable storage medium for high-level nuclear waste. Science (80-) 1984;226. https://doi.org/10.1126/science.226.4670.45.

[14] Sales BC, Boatner LA. Physical and chemical characteristics of lead-iron phosphate nuclear waste glasses. J Non Cryst Solids 1986;79:83–116. https://doi.org/10.1016/0022-3093(86)90040-2.

[15] Durville FM, Behrens EG, Powell RC. Laser-induced refractive-index gratings in Eu-doped glasses. Phys Rev B 1986;34. https://doi.org/10.1103/PhysRevB.34.4213.

[16] Liang X, Zhu C, Yang Y, Yuan S, Chen G. Luminescent properties of Dy3+-doped and Dy3+-Tm3+co-doped phosphate glasses. J Lumin 2008;128. https://doi.org/10.1016/j.jlumin.2007.11.086.

[17] El Jouad M, Bouabdalli EM, Touhtouh S, Addou M, Ollier N, Sahraoui B. Red

luminescence and UV light generation of europium doped zinc oxide thin films for optoelectronic applications. EPJ Appl Phys 2020;91. https://doi.org/10.1051/epjap/2020200133.

[18] Bouabdalli EM, El Jouad M, Garmim T, Touhtouh S, Louardi A, Monkade M, et al. Preparation and Characterization of Nickel and Aluminum-Codoped SnO2Thin Films for Optoelectronic Applications. Int J Photoenergy 2021;2021. https://doi.org/10.1155/2021/5556441.

[19] Bunker BC, Arnold GW, Wilder JA. Phosphate glass dissolution in aqueous solutions. J Non Cryst Solids 1984;64. https://doi.org/10.1016/0022-3093(84)90184-4.

[20] Ma L, Brow RK, Schlesinger ME. Dissolution behavior of Na2O–FeO–Fe2O3–P2O5 glasses. J Non Cryst Solids 2017;463. https://doi.org/10.1016/j.jnoncrysol.2017.02.022.

[21] Ramzi Z, Touhtouh S, Nachit W, Benkhouja K, Taibi M, Hajjaji A. Investigation of structural and physical properties of xSrO-(100-x)P2O5 glasses. Mol Cryst Liq Cryst 2016;627. https://doi.org/10.1080/15421406.2015.1137137.

[22] Hoppe U, Walter G, Kranold R, Stachel D. Structural specifics of phosphate glasses probed by diffraction methods: a review. J Non Cryst Solids 2000;263–264:29–47. https://doi.org/10.1016/S0022-3093(99)00621-3.

[23] Aguiar H, Solla EL, Serra J, González P, León B, Malz F, et al. Raman and NMR study of bioactive Na2O–MgO–CaO–P2O5–SiO2 glasses. J Non Cryst Solids 2008;354:5004–8. https://doi.org/10.1016/J.JNONCRYSOL.2008.07.033.

[24] Ibrahim AM, Badr AM, Elshaikh HA, Mostafa AG, Elbashar YH. Effect of CuO-addition on the Dielectric Parameters of Sodium Zinc Phosphate Glasses. Silicon 2018;10. https://doi.org/10.1007/s12633-017-9599-9.

[25] Goj P, Stoch P. Influence of CaO on structural features of polyphosphate P2O5-Fe2O3-FeO glasses by molecular dynamics simulations. J Non Cryst Solids 2020;537:120014. https://doi.org/10.1016/j.jnoncrysol.2020.120014.

[26] Todorov IT, Smith W, Trachenko K, Dove MT. DL_POLY_3: New dimensions in molecular dynamics simulations via massive parallelism. J Mater Chem 2006;16. https://doi.org/10.1039/b517931a.

[27] Bush IJ, Todorov IT, Smith W. A DAFT DL_POLY distributed memory adaptation of the Smoothed Particle Mesh Ewald method. Comput Phys Commun 2006;175:323–9. https://doi.org/10.1016/J.CPC.2006.05.001.

[28] Gao LW, Xia X Bin, Xu XQ, Chen CQ. Immobilization of radioactive fluoride waste in aluminophosphate glass: a molecular dynamics simulation. Nucl Sci Tech 2018;29. https://doi.org/10.1007/s41365-018-0443-8.

[29] Ben Slimen F, Haouari M, Ben Ouada H, Guichaoua D, Raso P, Bidault X, et al. Investigation of the local environment of Eu3+ in a silicophosphate glass using site-selective spectroscopy and Molecular Dynamics simulations. Opt Mater (Amst) 2017;64:479–88. https://doi.org/10.1016/j.optmat.2017.01.002.

[30] Goj P, Stoch P. Influence of CaO on structural features of polyphosphate P2O5-Fe2O3-FeO glasses by molecular dynamics simulations. J Non Cryst Solids 2020;537. https://doi.org/10.1016/j.jnoncrysol.2020.120014.

[31] Stoch P, Stoch A, Ciecinska M, Krakowiak I, Sitarz M. Structure of phosphate and iron-phosphate glasses by DFT calculations and FTIR/Raman spectroscopy. J Non Cryst Solids 2016;450. https://doi.org/10.1016/j.jnoncrysol.2016.07.027.

[32] Al-Hasni B, Mountjoy G. Structural investigation of iron phosphate glasses using molecular dynamics simulation. J Non Cryst Solids 2011;357:2775–9. https://doi.org/10.1016/j.jnoncrysol.2010.10.010.

[33] Hoppe U, Kranold R, Stachel D, Barz A, Hannon AC. Variation in P-O Bonding in Phosphate Glasses - A Neutron Diffraction Study. Zeitschrift Fur Naturforsch - Sect A J Phys Sci 2000;55. https://doi.org/10.1515/zna-2000-3-401.

[34] Hoppe U, Walter G, Kranold R, Stachel D. An X-ray Diffraction Study of the Structure of Vitreous P2O5. Zeitschrift Fur Naturforsch - Sect A J Phys Sci 1998;53. https://doi.org/10.1515/zna-1998-3-401.

[35] Wright AC, Sinclair RN, Shaw JL, Haworth R, Marasinghe GK, Day DE, et al. The atomic and magnetic structure and dynamics of iron phosphate glasses. Phys Chem Glas Eur J Glas Sci Technol Part B 2012;53.

[36] Stoch P, Goj P, Ciecińska M, Stoch A. Structural features of 19Al2O3-19Fe2O3-62P2O5 glass from a theoretical and experimental point of view. J Non Cryst Solids 2019;521. https://doi.org/10.1016/j.jnoncrysol.2019.119499.

[37] Stoch P, Szczerba W, Bodnar W, Ciecinska M, Stoch A, Burkel E. Structural properties of iron-phosphate glasses: Spectroscopic studies and ab initio simulations. Phys Chem Chem Phys 2014;16. https://doi.org/10.1039/c4cp03113j.

[38] Stoch P, Goj P, Wajda A, Stoch A. Alternative insight into aluminium-phosphate glass network from ab initio molecular dynamics simulations. Ceram Int 2021;47. https://doi.org/10.1016/j.ceramint.2020.09.018.

[39] Fan G, Diao J, Jiang L, Zhang Z, Xie B. Molecular dynamics analysis of the microstructure of the CaO-P2O5-SiO2 slag system with varying P2O5/SiO2 ratios. Mater Trans 2015;56. https://doi.org/10.2320/matertrans.M2014363.

[40] Christie JK, de Leeuw NH. Effect of strontium inclusion on the bioactivity of phosphate-based glasses. J Mater Sci 2017;52. https://doi.org/10.1007/s10853-017-1155-x.

[41] Johnson JA, Urquidi J, Holland D, Johnson CE, Appelyard PG. Strontium environment transition in tin silicate glasses by neutron and X-ray diffraction. J Non Cryst Solids 2007;353. https://doi.org/10.1016/j.jnoncrysol.2007.06.015.

[42] Goj P, Wajda A, Stoch P. Development of a new sr-o parameterization to describe the influence of sro on iron-phosphate glass structural properties using molecular dynamics simulations. Materials (Basel) 2021;14. https://doi.org/10.3390/ma14154326.

[43] Belashchenko DK, Ostrovskii OI. Computer simulation of noncrystalline P 2O 5, an ionic-covalent oxide. Inorg Mater 2002;38. https://doi.org/10.1023/A:1013603527862.

[44] Christie JK, Malik J, Tilocca A. Bioactive glasses as potential radioisotope vectors for in situ cancer therapy: Investigating the structural effects of yttrium. Phys Chem Chem Phys 2011;13. https://doi.org/10.1039/c1cp21764j.